AGU PUBLICATIONS

Geophysical Research Letters

RESEARCH LETTER
10.1002/2015GL064349

Key Points:
- Alaska mass balance is $-75 \pm 11/-16$ Gt yr-1 (1994–2013)
- Variability of response of individual glaciers to climate change is large
- Tidewater glaciers contributed only 6% to the mass balance of the region

Supporting Information:
- Text S1, Figures S1–S12, and Table S1

Correspondence to:
C. F. Larsen,
cflarsen@alaska.edu

Citation:
Larsen, C. F., E. Burgess, A. A. Arendt, S. O'Neel, A. J. Johnson, and C. Kienholz (2015), Surface melt dominates Alaska glacier mass balance, *Geophys. Res. Lett.*, *42*, doi:10.1002/2015GL064349.

Received 23 APR 2015
Accepted 2 JUN 2015
Accepted article online 4 JUN 2015

Surface melt dominates Alaska glacier mass balance

C. F. Larsen[1], E. Burgess[1,2], A. A. Arendt[3], S. O'Neel[2], A. J. Johnson[1], and C. Kienholz[1]

[1]Geophysical Institute, University of Alaska Fairbanks, Fairbanks, Alaska, USA, [2]Alaska Science Center, U.S. Geological Survey, Anchorage, Alaska, USA, [3]Polar Science Center, Applied Physics Laboratory, University of Washington, Seattle, Washington, USA

Abstract Mountain glaciers comprise a small and widely distributed fraction of the world's terrestrial ice, yet their rapid losses presently drive a large percentage of the cryosphere's contribution to sea level rise. Regional mass balance assessments are challenging over large glacier populations due to remote and rugged geography, variable response of individual glaciers to climate change, and episodic calving losses from tidewater glaciers. In Alaska, we use airborne altimetry from 116 glaciers to estimate a regional mass balance of -75 ± 11 Gt yr^{-1} (1994–2013). Our glacier sample is spatially well distributed, yet pervasive variability in mass balances obscures geospatial and climatic relationships. However, for the first time, these data allow the partitioning of regional mass balance by glacier type. We find that tidewater glaciers are losing mass at substantially slower rates than other glaciers in Alaska and collectively contribute to only 6% of the regional mass loss.

1. Introduction

Mountain glaciers represent <1% of the global glacier ice volume [*Meier et al*., 2007; *Vaughan et al*., 2013], but their rapid rate of mass loss accounts for nearly one third of the current observed sea level rise (SLR) [*Gardner et al*., 2013]. Under existing projections mountain glaciers will be a major contributor to the 21st century sea level budget. However, uncertainties are large [*Church et al*., 2013] due to a paucity of observations with which to calibrate models that predict surface mass balance (SMB, the sum of surface accumulation and ablation) as a function of climate. Existing models also ignore the impact of iceberg calving (calving herein refers to all flux through termini) on glacier mass loss. Simplified, worst-case scenarios show that glacier changes due to iceberg calving worldwide could outpace SMB losses by 2100 [*Meier et al*., 2007; *Church et al*., 2013], yet few observations exist to assess whether such an evolution is realistic.

The Alaska region, which we define to include the glaciers of Alaska, southwest Yukon Territory, and coastal northern British Columbia, is one of the largest mountain glacier contributors to SLR [*Gardner et al*., 2013]. Tidewater glaciers cover 14% of the total glacier area [*Pfeffer et al*., 2014; *Kienholz et al*., 2015] and are broadly assumed to be prone to dynamic instability and rapid retreat [*Arendt*, 2011]. Previous assessments of glacier mass balance for this region exist but have (1) neglected to partition individual glacier changes due to the lack of a comprehensive glacier inventory [*Berthier et al*., 2010], (2) used gravimetry data which are incapable of resolving or partitioning individual sources of glacier change [*Luthcke et al*., 2013], or (3) undersampled those glaciers with the potential for calving losses [*Arendt et al*., 2002]. Here we use airborne altimetry data from NASA's Operation IceBridge to directly assess patterns of glacier mass change in Alaska and investigate how SMB and calving dynamics contribute to mass losses.

2. Data and Analysis

The University of Alaska Fairbanks has flown lidar altimetry on glaciers in Alaska from 1994 to 2013 (Figure S1 in the supporting information). These surveys have been part of NASA's Operation IceBridge mission since 2009 [*Larsen*, 2010]. The basic observations consist of elevation profiles flown along glacier centerlines covering as much of each glacier's elevation range as is practical. When repeated at approximately the same date in subsequent years, the rate of elevation change is measured, and this is used to estimate mass balance over the elapsed interval. Survey flights target many small and most of the large glaciers in Alaska (Figure 1), and the aggregate hypsometry of surveyed glaciers covers much of the hypsometric

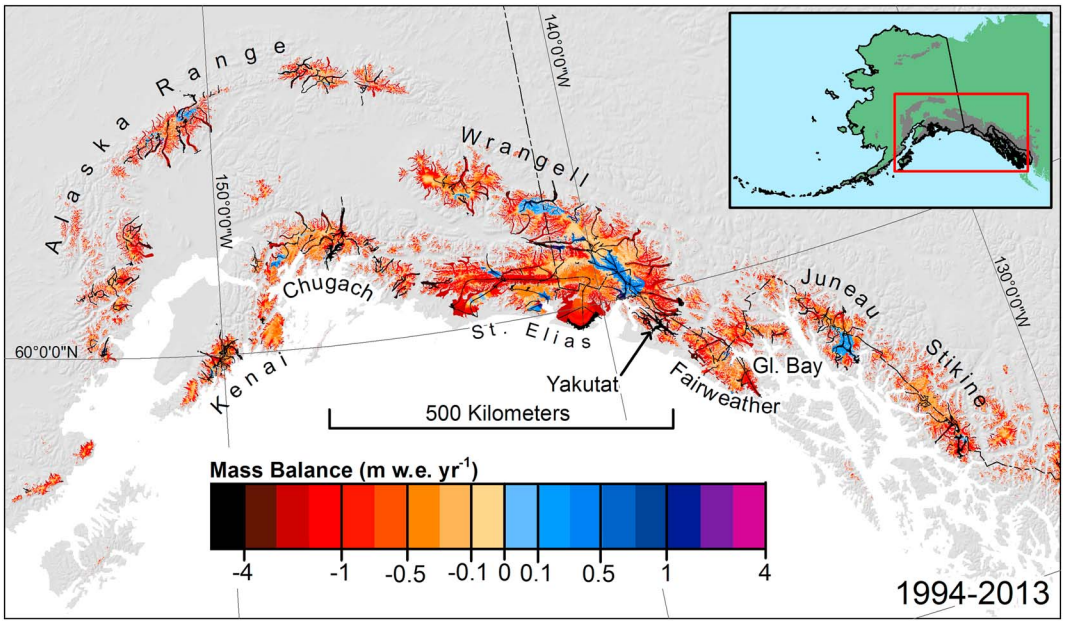

Figure 1. Estimated mass balance (1994–2013) for surveyed and unsurveyed glaciers in the most densely glacierized subregion of Alaska. The inset shows the entire region. Black lines indicate survey flight lines.

range of the entire Alaska region (Figure S6). Our data do not include any glaciers with areas $< 3\,km^2$, which account for ~16% of Alaska glacier area (Figure S5). This omission has potential to bias our regional mass balance estimate as we discuss in section 4.

Our surveys are scheduled close to the annual mass maximum in spring or the annual mass minimum in autumn, when the rate of seasonal mass change is near zero. Repeat surveys occur within an average of 8 days of the previous survey date (the maximum is 30 calendar days). Intervals between repeat surveys used herein are required to be a minimum of 5 years, with an average of 10 years (Figure S1). The intervals we use are centered on 2008 (Figure S2), owing to a steady increase in the number of surveys performed annually. We incorporate only the longest interval available for each glacier in our analysis, as this minimizes the impacts of seasonal elevation change, interannual variability, and uncertainties associated with snow and firn densification [*Huss*, 2013].

We estimate the total mass balance (B_a, expressed as an average annual mass balance rate in water equivalent units) of 116 glaciers (Table S1), representing 41% of Alaska's glacierized area. We integrate the measured rates of centerline elevation change over each surveyed glacier's hypsometry [*Johnson et al.*, 2013] using the Randolph Glacier Inventory (RGI; [*Pfeffer et al.*, 2014; *Kienholz et al.*, 2015]). We mitigate potential biases resulting from the use of centerline elevation changes as representative of glacier-wide changes [*Berthier et al.*, 2010] following *Johnson et al.* [2013] (see the supporting information). Volume change is converted to the glacier-wide mass balance (B_a) using a constant density of $850\,kg\,m^{-3}$ under the assumption of Sorge's law [*Huss*, 2013; *Johnson et al.*, 2013].

Our surveys cover 18 tidewater glaciers, accounting for 81% of Alaska's tidewater glacier area, and 32 lake-terminating glaciers, representing 68% of the total lake-terminating glacier area. We extrapolate to unsurveyed glaciers after subdividing the elevation change observations by terminus type (land-, lake-, and tidewater-terminating) and then determining the mean elevation change profiles for these three dynamical classes (Figure 2). We choose to parameterize elevation change as a function of elevation because of the dominant control of elevation-dependent climate gradients on mass balance distribution. Other regionalization approaches emphasize the role of glacier geometry as quantified by surface area or slope in controlling the collective response of glaciers to climate [*Harrison*, 2013; *Bahr et al.*, 2015], but the way in which these approaches apply to extrapolation of altimetry data has not yet been explored.

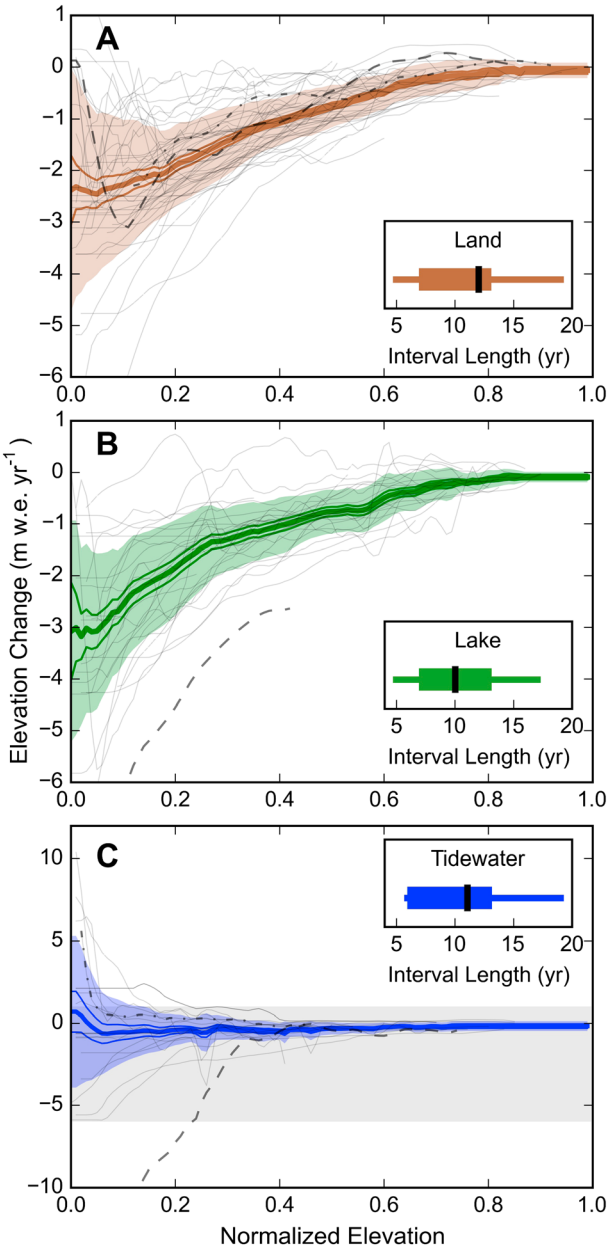

Figure 2. Surveyed centerline elevation change rate as a function of normalized elevation where zero is the glacier terminus and one the glacier head (grey lines). Thick and thin colored lines represent mean elevation change and standard error of the mean, respectively. Shaded areas indicate 1σ variability. Horizontal box plots show the distribution of interval lengths, including the median (black), interquartile range (box size), and 5–95 percentiles of the intervals. (a) Land-terminating glaciers. Dashed line is Gulkana Glacier, and dot dash is Wolverine Glacier. (b) Lake-terminating glaciers. Dashed line is Yakutat Glacier. (c) Tidewater glaciers. Dashed line is Columbia Glacier, and dot-dash is Hubbard Glacier. The expanded *y* axis for Figure 2c relative to Figures 2a and 2b is required to capture variability near the termini of these glaciers. The range of Figures 2a and 2b is indicated with the grey shading in Figure 2c.

To construct the mean elevation change profiles for each dynamical class of glacier (Figure 2), we normalize each glacier's elevation change profile by the maximum and minimum elevation of that glacier:

$$z_{\mathrm{norm}} = (z - z_{\mathrm{min}})/(z_{\mathrm{max}} - z_{\mathrm{min}})$$

where z_{min} and z_{max} are the elevations of the glacier terminus and head [*Johnson et al.*, 2013]. This normalization allows comparison and averaging of elevation changes across all glacier sizes and elevation distributions [*Johnson et al.*, 2013]. Using the nonparametric Mann-Kendall test, we find no statistically significant relationship between glacier minimum glacier elevation and mass balance ($p = 0.78$). However, we do observe a characteristic pattern of elevation changes over each glacier's elevation range. These observations encourage stacking of the normalized elevation change profiles to characterize average elevation changes (Figures S8–S10 in the supporting information). Prior to averaging the profiles, a terminus correction is applied for all retreating glaciers (Figure S11). We omit Columbia Glacier, Yakutat Icefield glaciers, and all surge-type glaciers when deriving mean profiles to minimize the influence of anomalous dynamics on the extrapolation. Our extrapolation extends to all glaciers in the Alaska region of version 4.0 of the RGI [*Kienholz et al.*, 2015].

We estimate the mass balance of each unmeasured glacier by (i) selecting the glacier's outline from the RGI inventory [*Kienholz et al.*, 2015], (ii) choosing the normalized mean elevation change profile associated with that glacier's dynamical type, (iii) extracting the hypsometry for that glacier and normalizing it by elevation as defined above, and (iv) integrating the mean elevation change profile over the normalized glacier hypsometry. We treat each glacier individually in this extrapolation, avoiding the use of aggregate hypsometries of unsurveyed glacier area as was done in previous studies [*Johnson et al.*, 2013; *Das et al.*, 2014]. This treatment allows us to properly account for individual glacier geometries and the distribution of elevation changes along their profiles. The importance of doing this summation correctly over the extrapolated area is

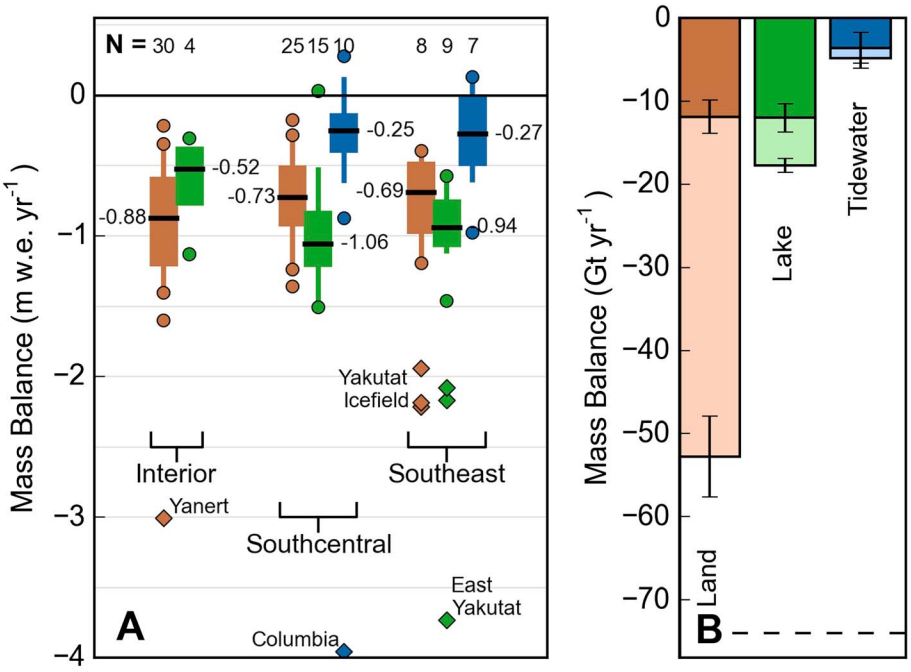

Figure 3. Mass balance distributions and partitioning. (a) Box plots for surveyed glacier mass balance, grouped by climate region and terminus type. Boxes represent the interquartile range (25th to 75th percentiles), with an annotated horizontal line at the median value. Whiskers extend to the 5th and 95th percentiles. Outliers are shown with circles. Diamonds show surveyed glaciers with anomalous behavior that are excluded from the distributions shown by the boxplots. Brown, green, and blue indicate land-, lake-, and tidewater-terminating glaciers, respectively. Sample size (*N*) is given above each boxplot. The interior climate region includes the Wrangell and Alaska ranges. The south central climate region includes the Kenai, Chugach, and St. Elias ranges, and the southeast region includes Yakutat Icefield, Glacier Bay, and Juneau and Stikine icefields. See Figure 1 for locations. (b) Regional mass balance of surveyed (darker shading) and unsurveyed glaciers (lighter shading) for the three terminus types. Uncertainties are 1σ. Horizontal dashed line indicates the estimated total regional balance (-75 Gt yr^{-1}).

significant. If we instead integrate the mean profiles for land-, lake-, and tidewater-terminating glaciers over aggregate hypsometries of unsurveyed areas of each respective glacier type, then the mass balance of the Alaska region is overestimated by 41%. Subdividing the unsurveyed area into subregions with similar hypsometries as was done in previous studies [*Johnson et al.*, 2013; *Das et al.*, 2014] likely reduces uncertainties from using aggregate hypsometries but to what degree is unclear.

3. Results

Our analysis yields a mass balance of -75 ± 11 Gt yr^{-1} for the Alaska region (Figure 3). The tidewater glacier mass balance is -5 ± 3 Gt yr^{-1}. Columbia Glacier contributes -4 ± 0.3 Gt yr^{-1}, and the remaining 48 tidewater glaciers in Alaska have an estimated mass balance of only -1 ± 3 Gt yr^{-1}. Lake-terminating glaciers comprise 20% of the Alaska glacier area and contribute 24% to the total mass loss ($B_a = -17 \pm 2$ Gt yr^{-1}). The remaining 70% of Alaska glacier mass loss is attributable to land-terminating glaciers ($B_a = -53 \pm 6$ Gt yr^{-1}), which tend to show steady change more directly coupled and proportional to variations in climate. Our total mass budget agrees well with existing regional estimates, including those using Ice, Cloud, and land Elevation Satellite (-65 ± 12 Gt yr^{-1}) [*Arendt et al.*, 2013] and Gravity Recovery and Climate Experiment (GRACE) (-76 ± 4 Gt yr^{-1} and -69 ± 11 Gt yr^{-1}) [*Sasgen et al.*, 2012; *Luthcke et al.*, 2013], as well as a 2003–2009 consensus estimate that combined GRACE, field measurements, and earlier airborne altimetry (-50 ± 17 Gt yr^{-1}) [*Gardner et al.*, 2013]. Our estimate is significantly more negative than one GRACE estimate (-42 ± 6 Gt yr^{-1}) [*Jacob et al.*, 2012]. Our uncertainties are smaller than those of a previous University of Alaska Fairbanks (UAF) altimetry study ($B_a = -96 \pm 35$ Gt yr^{-1}) [*Arendt et al.*, 2002] for the 1995–2001 period, which had fewer surveyed glaciers (28 versus 116) and extrapolated to unsurveyed glaciers using an incomplete glacier inventory. Limiting the extrapolation to the area in *Arendt et al.* [2002] reduces our estimate to -71 Gt yr^{-1}.

Partitioning the data set by dynamical class isolates the largest observed systematic variations in surface elevation change, while keeping each sample large enough to provide a robust mean profile. Alternatives to this dynamic-based partitioning, including an all-inclusive extrapolation, geographic [*Arendt et al*., 2009] and climate-based partitioning, and combinations thereof are examined in Figure S12. These differences in partitioning methods perturb the regional mass balance estimate by <10% (Figure S12A). This sensitivity testing also highlights that tidewater glaciers have mass balances significantly different from all other groupings of glaciers regardless of the partitioning approach (Figure S12B). We also test the effect of using different minimum interval lengths from 4 to 10 years (Figure S12). Requiring a 10 year interval length reduces our sample size by ~40% but only affects the regional mass balance by 7%, which suggests that glacier-to-glacier elevation changes are highly stochastic in nature.

4. Discussion

We observe large glacier-to-glacier variations in elevation change rates (Figure 2), which lead to large variations in glacier mass balance (Figure 3). Considering only surveyed land-terminating, nonsurge type glaciers, we find the standard deviation of mass balance is 0.54 meters water equivalent (mwe) yr^{-1}, more than half the magnitude of their regional average mass balance. We find similarly broad distributions of mass balances for land-, lake-, and tidewater-terminating glaciers. The greatest variability in elevation change rates is near tidewater termini, where the standard deviation of elevation change exceeds 5 mwe yr^{-1}, nearly double that of the land- and lake-terminating termini. However, over the upper 80% of the profile (Figure 2), tidewater glacier elevation change variability is similar (within 10%) to the along-profile variability of land- and lake-terminating glaciers at corresponding elevations. While our measurement intervals are not all coincident, temporal variability is unlikely to be responsible for the large mass balance variability observed (Figures S3 and S4 in the supporting information). Rather, we find that the majority of the variability we observe is not spatially autocorrelated and results from persistent glacier-to-glacier differences in mass balance. This variability is large enough to preclude the detection of patterns in mass balance resulting from climate variability, continentality, or latitude, despite our observations spanning roughly 1300 km and a range of climates.

Nonetheless, amidst this large random variability, we find faster rates of land-terminating mass loss in the interior than in coastal subregions (Figure 3a) ($p = 0.05$) (see the supporting information). This observation is opposite from findings by *Berthier et al*. [2010], who found slower rates of mass loss in the interior than on the coast for the period 1962–2006, but is in agreement with basin-scale field observations [*O'Neel et al*., 2014]. Furthermore, we find land-terminating glacier mass balance to be significantly ($p = 0.01$) correlated to glacier size (Figure S5), exhibiting more negative values on smaller glaciers. This finding supports a recent global consensus report [*Gardner et al*., 2013] that suggested that field programs have oversampled small glaciers and biased global mountain-glacier SLR estimates. Conversely, our data set preferentially targets large glaciers due to their greater SLR potential. We estimate that this sampling bias could lead us to underestimate regional mass loss by 5 Gt yr^{-1} (see the supporting information).

It is reasonable to assume that the observed differences in glacier mass balances are driven by glacier geometry and local climate variability, but over what range of scales do these parameters become important? Meteorological station data show some regional homogeneity in temperature and precipitation variability but with distinct differences on either side of topographic divides [*Bieniek et al*., 2012]. Alaska's glaciers are positioned on these topographic divides and thus occupy transitional climate zones with complex climate patterns that deviate from regional averages. Highly variable climate in these alpine zones likely contributes to the large glacier-to-glacier variability we observe, even among neighboring glaciers. In addition, an individual glacier's thickness, slope, and hypsometry combine in complex ways to produce different response times to a given climate signal, and the slope and aspect of glaciers and their surrounding topography create spatial variability in radiation budgets and surface mass balance [*Harrison*, 2013; *Bahr et al*., 2015]. If such factors are indeed the principle drivers of the variability observed, then mass balance models may need to carefully address basin-scale details and parameterization.

Dynamic drivers of mass loss associated with calving glaciers add further complexity to our assessment of mass balance variability. Many surveyed lake-terminating glaciers show more rapid thinning near their termini than observed on land-terminating glaciers (Figure 2a). Median mass balance rates for lake-terminating glaciers are

more negative in coastal regions where large, well-developed proglacial lakes exist (Figure 3a). These lakes are indicative of substantial overdeepenings along the glacier beds near these termini, a geometry that can lead to dynamic instabilities similar to those found at tidewater glaciers. Even in the absence of significant iceberg calving, large proglacial lakes impede these glaciers from achieving equilibrium simply because the terminus is held at the elevation of the lake until the retreat is clear of the overdeepening [*Mercer*, 1961]. The combined impact of these effects can be very large; Yakutat Glacier is second only to Columbia Glacier for the most negative mass balance among the glaciers we surveyed. Yakutat Glacier terminates in an unusually long overdeepening, which amplifies these effects [*Trüssel et al*., 2013]. The majority of lake-terminating glaciers we surveyed does not exhibit such extremely rapid mass loss (Table S1). At present, the Yakutat Icefield system is an outlier within our observations of lake-terminating glaciers.

Despite the negligible collective mass loss from the tidewater glaciers (excluding Columbia), 14 of the 18 surveyed tidewater glaciers exhibit a negative mass balance (Table S1). Excluding Columbia, LeConte, and those with positive mass balance, mass balances for the remaining 12 surveyed glaciers are small in magnitude, only -0.3 ± 0.3 mwe yr^{-1} as compared to -0.9 ± 0.1 mwe yr^{-1} for land- and lake-terminating glaciers. The four tidewater glaciers gaining mass have a collective mass balance of $+0.5 \pm 0.9$ Gt yr^{-1} and thus offset some of the regional tidewater mass loss. Seven of the surveyed tidewater glaciers are advancing [*McNabb and Hock*, 2014], but five of these have negative mass balances due to upstream thinning, demonstrating that advance does not necessarily imply mass gain. Over centurial timescales, advance and retreat of these grounded, temperate glaciers follow the aperiodic and partially unstable "tidewater glacier cycle" [*Post et al*., 2011]. Almost all of Alaska's tidewater glaciers are now in a "retracted stable" phase of this cycle [*Post et al*., 2011; *McNabb and Hock*, 2014] following widespread dynamic retreat since the end of the Little Ice Age. This configuration, which occurs after the loss of significant portions of the ablation area, tends to favor mass gain under steady climate conditions [*Post et al*., 2011]. Despite this, our observations show that the majority of tidewater glacier mass balances are negative, suggesting that the climate has warmed enough to retard the onset of the advance phase of the tidewater glacier cycle.

Over the period 1994–2013, Alaska's tidewater glaciers contributed only 6% of Alaska's mass loss, establishing that rapid tidewater glacier retreat is not a primary control on regional mass loss. Tidewater glaciers here are now less vulnerable to future catastrophic retreat than they have been at any time since the end of the Little Ice Age. However, several large, coastal glaciers with broad areas of ice grounded below sea level (Malaspina, Hubbard, Bering, and Taku) remain potentially susceptible to future calving instability. The scale of any such retreat could be substantial, as best demonstrated in Alaska by Glacier Bay's post-Little Ice Age 10 mm SLR contribution [*Motyka et al*., 2007]. With no such evolution imminent, our results now turn attention to surface melt as the more predictable and ultimately more certain mechanism of Alaska's future mass loss.

The rate of surface mass loss we observe on nontidewater glaciers is extremely high, comparable to mass loss rates at lower latitudes [*Gardner et al*., 2013]. Regional losses are occurring at nearly double the rate found over the period 1962–2006 [*Berthier et al*., 2010]. Models suggest that SMB losses will not decline [*Radić and Hock*, 2011]. At these rates, Alaska contributed as much to SLR every 5 years (~1 mm) as the entire 35 year retreat of Columbia Glacier [*O'Neel et al*., 2005]. Despite Greenland's ice covered area being 20 times greater than that of Alaska, losses in Alaska were fully one third of the total loss from the ice sheet during 2005–2010 [*Vaughan et al*., 2013]. Even if Alaska's large-scale tidewater glacier losses are now a relic of the past, Alaska will continue to be a primary contributor to global SLR through the end of this century. Although a diminished impact of tidewater instability on Alaska glacier mass balance improves the predictability of future changes, ultimately the dominance of surface mass balance will result in more widespread wastage of these glaciers under a warming climate.

Acknowledgments

This study is dedicated to Keith Echelmeyer; pilot, mountaineer, naturalist, pioneer glaciologist, and cofounder of the Alaska glacier altimetry program. Program cofounder Will Harrison provided helpful discussion and reviews. Detailed and insightful reviews by Graham Cogley and Erik Ivins improved the manuscript tremendously. We thank Paul Claus and Ultima Thule Lodge for flight support. C. Larsen, E. Burgess, and A. Johnson were funded by NASA NNX13AD52A. A. Arendt was funded by NASA NNX15AG21G. C. Kienholz was funded by NASA NNX11AF41G. S. O'Neel and E. Burgess were funded by the U.S. Geological Survey Climate and Land Use Research and Development Program and the Alaska Climate Science Center. For access to data see NSIDC: http://nsidc.org/data/icebridge/data_summaries.html.

The Editor thanks J. Graham Cogley and an anonymous reviewer for their assistance in evaluating this paper.

References

Arendt, A. A. (2011), Assessing the status of Alaska's glaciers, *Science*, *332*(6033), 1044–1045, doi:10.1126/science.1204400.

Arendt, A. A., K. A. Echelmeyer, W. D. Harrison, C. S. Lingle, and V. B. Valentine (2002), Rapid wastage of Alaska glaciers and their contribution to rising sea level, *Science*, *297*(5580), 382–386, doi:10.1126/science.1072497.

Arendt, A., J. Walsh, and W. Harrison (2009), Changes of glaciers and climate in Northwestern North America during the late twentieth century, *J. Clim.*, *22*(15), 4117–4134, doi:10.1175/2009JCLI2784.1.

Arendt, A., S. Luthcke, A. Gardner, S. O'Neel, D. Hill, G. Moholdt, and W. Abdalati (2013), Analysis of a GRACE global mascon solution for Gulf of Alaska Glaciers, *J. Glaciol.*, *59*(217), 913–924, doi:10.3189/2013JoG12J197.

Bahr, D. B., W. T. Pfeffer, and G. Kaser (2015), A review of volume-area scaling of glaciers, *Rev. Geophys.*, *53*, 1–46, doi:10.1002/2014RG000470.
Berthier, E., E. Schiefer, G. K. C. Clarke, B. Menounos, and F. Rémy (2010), Contribution of Alaskan glaciers to sea-level rise derived from satellite imagery, *Nat. Geosci.*, *3*(2), 92–95.
Bieniek, P. A., et al. (2012), Climate divisions for Alaska based on objective methods, *J. Appl. Meteorol. Climatol.*, *51*(7), 1276–1289, doi:10.1175/JAMC-D-11-0168.1.
Church, J. A., P. U. Clark, A. Cazenave, and J. M. Gregory (2013), Sea level change, in *Climate Change 2013: The Physical Science Basis. Contribution of Working Group I to the Fifth Assessment Report of the Intergovernmental Panel on Climate Change*, pp. 1137–1216, Cambridge Univ. Press, Cambridge, U. K., and New York.
Das, I., R. Hock, E. Berthier, and C. S. Lingle (2014), 21st-century increase in glacier mass loss in the Wrangell Mountains, Alaska, USA, from airborne laser altimetry and satellite stereo imagery, *J. Glaciol.*, *60*(220), 283–293, doi:10.3189/2014JoG13J119.
Gardner, A. S., et al. (2013), A reconciled estimate of glacier contributions to sea level rise: 2003 to 2009, *Science*, *340*(6134), 852–857, doi:10.1126/science.1234532.
Harrison, W. D. (2013), How do glaciers respond to climate? Perspectives from the simplest models, *J. Glaciol.*, *59*(217), 949–960, doi:10.3189/2013JoG13J048.
Huss, M. (2013), Density assumptions for converting geodetic glacier volume change to mass change, *Cryosphere*, *7*(3), 877–887, doi:10.5194/tc-7-877-2013.
Jacob, T., J. Wahr, W. T. Pfeffer, and S. Swenson (2012), Recent contributions of glaciers and ice caps to sea level rise, *Nature*, *482*(7386), 514–518, doi:10.1038/nature10847.
Johnson, A. J., C. F. Larsen, N. Murphy, A. A. Arendt, and S. Lee Zirnheld (2013), Mass balance in the Glacier Bay area of Alaska, USA, and British Columbia, Canada, 1995–2011, using airborne laser altimetry, *J. Glaciol.*, *59*(216), 632–648, doi:10.3189/2013JoG12J101.
Kienholz, C., S. Herreid, J. L. Rich, A. A. Arendt, R. Hock, and E. Burgess (2015), Derivation and analysis of a complete modern-date glacier inventory for Alaska and northwest Canada, *J. Glaciol.*, *61*(227), 403–420.
Larsen, C. (2010), IceBridge UAF Lidar Scanner L1B Geolocated Surface Elevation Triplets, NASA National Snow and Ice Data Center Distributed Active Archive Center, Boulder, Colo, doi:10.5067/AATE4JJ91EHC. [Updated 2014.]
Luthcke, S. B., T. J. Sabaka, B. D. Loomis, A. A. Arendt, J. J. McCarthy, and J. Camp (2013), Antarctica, Greenland and Gulf of Alaska land-ice evolution from an iterated GRACE global mascon solution, *J. Glaciol.*, *59*(216), 613–631.
McNabb, R. W., and R. Hock (2014), Alaska tidewater glacier terminus positions, 1948–2012, *J. Geophys. Res. Earth Surf.*, *119*, 153–167, doi:10.1002/2013JF002915.
Meier, M. F., M. B. Dyurgerov, U. K. Rick, S. O'Neel, W. T. Pfeffer, R. S. Anderson, S. P. Anderson, and A. F. Glazovsky (2007), Glaciers dominate eustatic sea-level rise in the 21st century, *Science*, *317*(5841), 1064–1067, doi:10.1126/science.1143906.
Mercer, J. H. (1961), The response of fjord glaciers to changes in the firn limit, *J. Glaciol.*, *3*(29), 850–858.
Motyka, R. J., C. F. Larsen, J. T. Freymueller, and K. A. Echelmeyer (2007), *Post Little Ice Age Glacial Rebound in Glacier Bay National Park and Surrounding Areas*, Alaska Park Science, Lakewood, Colo.
O'Neel, S., W. T. Pfeffer, R. Krimmel, and M. Meier (2005), Evolving force balance at Columbia Glacier, Alaska, during its rapid retreat, *J. Geophys. Res.*, *110*, F03012, doi:10.1029/2005JF000292.
O'Neel, S., E. Hood, A. Arendt, and L. Sass (2014), Assessing streamflow sensitivity to variations in glacier mass balance, *Clim. Change*, *123*(2), 329–341, doi:10.1007/s10584-013-1042-7.
Pfeffer, W. T., A. A. Arendt, A. Bliss, T. Bolch, J. G. Cogley, A. S. Gardner, J. O. Hagen, R. Hock, G. Kaser, and C. Kienholz (2014), The Randolph Glacier Inventory: A globally complete inventory of glaciers, *J. Glaciol.*, *60*(221), 537–552.
Post, A., S. O'Neel, R. J. Motyka, and G. Streveler (2011), A complex relationship between calving glaciers and climate, *Eos Trans. AGU*, *92*(37), 305–306, doi:10.1029/2011EO370001.
Radić, V., and R. Hock (2011), Regionally differentiated contribution of mountain glaciers and ice caps to future sea-level rise, *Nat. Geosci.*, *4*(2), 91–94, doi:10.1038/ngeo1052.
Sasgen, I., V. Klemann, and Z. Martinec (2012), Towards the inversion of GRACE gravity fields for present-day ice-mass changes and glacial-isostatic adjustment in North America and Greenland, *J. Geodyn.*, *59–60*, 49–63, doi:10.1016/j.jog.2012.03.004.
Trüssel, B. L., R. J. Motyka, M. Truffer, and C. F. Larsen (2013), Rapid thinning of lake-calving Yakutat Glacier and the collapse of the Yakutat Icefield, southeast Alaska, USA, *J. Glaciol.*, *59*(213), 149–161, doi:10.3189/2013J0G12J081.
Vaughan, D. G., J. Comiso, I. Allison, and J. Carrasco (2013), Observations: Cryosphere, in *Climate Change 2013: The Physical Science Basis. Contribution of Working Group I to the Fifth Assessment Report of the Intergovernmental Panel on Climate Change*, pp. 317–382, Cambridge Univ. Press, Cambridge, U. K., and New York.